Hermite transform based algorithm for detection and classification of high impedance faults

DANIEL GUILLEN[1], (Member, IEEE), JIMENA OLVERES[2], VICENTE TORRES-GARCIA, (Senior Member, IEEE), and BORIS ESCALANTE-RAMIREZ[2]

[1]Tecnologico de Monterrey, Escuela de Ingeniería y Ciencias, Monterrey, N.L., México.
[2]Universidad Nacional Autónoma de México, Facultad de Ingeniería, Coyoacán, Ciudad de México, México.

Corresponding author: Jimena Olveres(e-mail: jolveres@cecav.unam.mx).

ABSTRACT This work proposes a new algorithm to cope with the classification of high impedance faults (HIFs) in distribution systems because any HIF can be represented by small current magnitudes with non-linear variations, which complicate its detection in distribution grids. The proposed method uses the Hermite transform (HT) because this signal processing technique offers several advantages, one of which is associated with the multiple resolution levels resulting from the filter functions and the analysed electrical signal. The Hermite coefficients will depend on the filter functions where the filters help extract the most essential high frequency components aiming to identify the transient behaviour of HIFs. The processing of HIF signals allows identifying the main features regarding other transient events and typical faults. In this sense, to classify different types of faults and HIFs, a multiresolution approach based on the Hermite transform (HT) is proposed. The analysis is carried in a distribution network considering distributed generation, and all findings are discussed using three different classifiers, which are also compared against the discrete wavelet transform (DWT); the discussed results show that the proposed approach presents better performance during the discrimination of HIFs from typical faults.

INDEX TERMS Classification, Distribution grids, Fault detection, Hermite transform, High impedance faults, Multiresolution analysis.

NOMENCLATURE

H_n	Hermite polynomials
L_n	Hermite-expansion coefficients
D_n	Filter functions
$G(x)$	Gaussian window
$i(x)$	Electrical signal
v	Arc voltage
i	Arc current
τ	Time constant
$g(t)$	Arc conductance
$P(v, i)$	Arc power in steady-state
I_a, I_b, I_c	Line currents
$I_{HTa}, I_{HTb}, I_{HTc}$	High-frequency components
F_1	Standard deviation
F_2	Average absolute magnitude
F_3	Average energy
F_4	Kurtosis index

I. INTRODUCTION

THE aim of any distribution system (DS) is to supply the energy demanded by all possible customers. The grid congestion and the distances associated with the power distribution expose the grid to critical conditions such as faults and abnormal scenarios, which may affect the power quality and the system reliability. In this context, the protection systems must be reliable to detect faults as fast as possible to avoid large interruptions of load. One of the main existing issues of the distribution grids is the protection against short circuits that produce high current magnitudes resulting from "low impedance fault (LIFs)". However, in some cases, the fault may present small current magnitudes originated by "high impedance faults (HIFs)", which are characterized by a nonlinear behavior [1], [2]. Therefore, the correct discrimination between LIFs and HIFs has been an essential subject of interest because HIFs may present complex transient behaviour that complicate their detection. A HIF occurs when an overhead conductor makes contact with any object that hosts a path to ground. Due to the small

current magnitudes and the nonlinearity of the phenomenon, HIFs may not be detected by conventional overcurrent protections [3]. As a consequence of that, HIF detection has been studied using different signal processing techniques that may show the transient information associated with the electric arc phenomenon. The arc phenomenon is non-linear, asymmetric, and unpredictable that makes more complex the HIF detection in distribution grids. In fact, several studies have been carried out by analysing the patterns of the voltage and current signals aiming to find the HIF characteristics.

In general, the analysis of HIFs can be carried out in time, frequency, or time-frequency domains where the feature exploration is developed by advanced signal processing and artificial intelligence techniques. For instance, in [4] a methodology based on the harmonic content has been implemented, where the detection uses odd and even harmonics of the current signal to distinguish HIFs from other transient phenomena. In the same way, another proposal has been discussed in [5]; this method evaluates the even harmonics into the voltage waveform by using smart meters (SMs). In [6] the incorporation of inter-harmonic components superimposed into the current of conventional protections such as automatic recloser, and sectionalizer is analyzed demonstrating that this method facilitates the detection due to the variations found in the inter-harmonics. Following the same basis of inter-harmonics, the complex nature of HIFs has motivated to develop new proposals using multiresolution approaches; for instance, in [7] a proposal combines two techniques such as maximum overlap discrete wavelet packet transform (MODWPT) and empirical mode decomposition (EMD), demonstrating effective outcomes during the detection and classification of HIFs.

Due to the nonlinear behaviour and the intermittency of the electric arc, the current waveforms present asymmetries that can be detected by multiresolution techniques. For example, a simplified version of the DWT is employed, which uses the energy of the wavelet coefficients [8], [9]; HIF detection is carried out using a sliding window of one cycle of the fundamental frequency, which is validated with several surfaces when HIFs take place into the distribution grid. In the same way, in [10] a DWT-based method is introduced that monitors the high- and low-frequency components of voltage through the system. Another way to deal with HIFs in distribution networks is based on power spectral density (PSD) resulting from a multiresolution analysis by using the DWT [11], where the detection and classification process is carried out in a radial distribution system. In [12] a DWT-based ensemble Random Subspace (RS) classifier is proposed for discriminating HIFs in distribution grids with a photovoltaic system, where other three classifiers are employed such as K-nearest neighbour (KNN), logistic regression (LR), and random tree (RT) showing their effectiveness during the classification process of HIFs.

Other techniques such as mathematical morphology, empirical mode decomposition, and morphological gradient have been employed for HIFs detection and classification [13]–[16]. In [14], a multistage morphological-based fault detector is proposed to cope with HIFs in distribution systems by extracting the nonlinear features of HIFs. On the other hand, the EMD-based method proposed in [15] uses voltage signals to identify the predominant harmonic components, and the classification is performed by applying an artificial neural network (ANN). In the same context, in [17] a multilayer perceptron (MLP) artificial neural network (ANN) is proposed; in that proposal, the classification method is based on higher-order statistics (HOS), which is also combined with Fisher's discrimination ratio for extracting specific patterns associated with the HIFs. The multi-resolution morphological gradient (MMG) method has also been proved to be an effective tool for discriminating HIFs from other transient phenomena [16]. That method consists of analysing the fault currents to extract the main features that are used as inputs to a multi-layer perceptron neural network. Therefore, the detection will depend on the feature extraction used in the classifier and the data set. In the same context, a classifier named boosted decision trees (BDT) has been applied in HIFs [18]; the proposed method employs the high-frequency components and is performed through real data set comprising a large number of experiments that are also assessed in the presence of noise. Another approach based on time-frequency analysis is proposed using a support vector machine (SVM) classifier [19]. A similar application of SVM is reported in [20], which is combined with Principal Component Analysis (PCA) to cope with the detection and classification of HIFs.

On the other hand, other techniques based on time-domain analysis have been introduced [21], [22]. For instance, in [21] the superimposed high-frequency components of voltages and currents are analyzed using the moving sum of one cycle of the fundamental frequency. Besides, a time-domain approach focusing on fault location based on a linear least square-based estimator is also applied in [22]. In general, the limitations and advantages of all different applied methods depend on the signal processing techniques employed and the feature extraction process, which will define the effectiveness of any classifier. In this sense, this paper proposes a new method based on the Hermite transform (HT), which offers several coefficients of resolution in only one scale of analysis.

The main contribution of this work is the development of a new method able to discriminate typical faults from HIFs in distribution networks by including distributed generation. The method employs a multiresolution analysis following the fundamentals of the HT, which takes into account different resolution levels, and at the same time presents adaptability since each filter function resonances in different proportions regarding the electrical signal under study. Therefore, the method offers large capabilities during the feature extraction that is the key to getting successful results during the discrimination process. The classification process is mainly developed using four different characteristics defined by the high-frequency components. This proposed scheme is assessed by employing three different classifiers KNN, SVM, and NN. In

addition, the obtained results are verified through comparison results with the DWT.

II. HIGH IMPEDANCE FAULTS MODELLING AND ANALYSIS

A. HERMITE TRANSFORM

The Hermite transform is an efficient signal processing tool that is also used for examining electrical signals (voltage or current signals). The main transient components of any electrical signal $i(x)$ can be extracted by expanding the signal following a decomposition process defined by the Hermite polynomials [23]. The decomposition of the signal $i(x)$ is carried out by using a sliding a Gaussian window $G(x - kT)$ at overlapping positions, which can be expressed in the time domain as follows:

$$G(x - kT)\left[i(x) - \sum_{n=0}^{\infty} L_n(kT) H_n(x - kT) \right] = 0 \quad (1)$$

where $H_n(x)$ corresponds to the Hermite polynomials, whereas $L_n(kT)$ stands for the expansion coefficients.

The Hermite polynomials $H_n(x)$ build an orthogonal basis with respect to a Gaussian window. Therefore, the expansion coefficients can be obtained with [23]:

$$L_n(kT) = \int_{-\infty}^{\infty} i(x) H_n(x - kT) G^2(x - kT) \, dx \quad (2)$$

Expression (2) shows the polynomial expansion coefficients $L_n(kT)$ of a signal $i(x)$; in fact, the coefficients $L_n(kT)$ can be computed through a convolution between the filter functions $D_n(x)$ and the studied signal $i(x)$. Notice that the process is followed by a subsampling process at multiple positions of T, and the filter functions $D_n(x)$ are represented by:

$$D_n(x) = H_n(-x) G^2(-x) \quad (3)$$

The filter function of order n corresponds to the $n - th$ derivative of a Gaussian function, and each filter function of order n can be represented by [23]:

$$D_n(x) = \frac{1}{\sqrt{2^n n!}} \frac{d^n}{d\left(\frac{x}{\sigma}\right)^n} \left[\frac{1}{\sigma\sqrt{\pi}} e^{\left(-\frac{x^2}{\sigma^2}\right)} \right] \quad (4)$$

On the other hand, the subsampling period T is a free parameter with the only restriction that the adjacent Gaussian windows must be overlapped.

The HT presents several advantages over other decomposition schemes. One of the most relevant advantages is its optimal location property in time-frequency based on the uncertainty principle. Besides, each Gaussian window represents a function that guarantees no spurious artifacts in the resulting analyzed signals. Additionally, the analysis filters (Gaussian derivatives) have proven to be efficient feature detectors. The multiscale analysis of the studied signal can be performed by systematically increasing the Gaussian window

width; this process allows detecting any transient component (frequency components) at different time scales [24], [25].

From a practical point of view, digital signals require discrete computation, so the discrete Hermite transform should be formulated and two approaches can be used according to [23]. The first one consists of approximating the filter functions by finite support filters; the second one uses a discrete polynomial expansion, that is, the continuous Hermite polynomials are approximated by discrete polynomials (Krawtchouk polynomials), which are orthogonal regarding the binomial window function, which in turn corresponds to an approximation of a Gaussian window. Both approaches allow getting similar results, and the first one is chosen to analyse the studied signals in this work.

For applications in distribution systems, the line currents of a specific protected distribution line are sampled and these are processed using the HT to discriminate LIF from HIF. Once the current signals are sampled, these are analysed by expanding each signal according to the HT approach, and the produced Hermite coefficients $L_n(kT)$ can be employed to find the most significant features aiming at discriminating HIFs from typical faults. The time-frequency features of the HIF signals can be efficiently detected by changing the spread of the analysis function (Gaussian function) due to its optimal location as argued before.

B. MODELLING OF HIGH IMPEDANCE FAULTS

HIFs in distribution grids are frequently composed of non-linear characteristics coming from an electric arc and the contact surface, these are responsible for developing small current magnitudes, a non-linear dependency between voltages and currents, and asymmetric current waveforms. These characteristics can be used to develop HIF models. The behaviour of HIFs can be understood using a non-linear resistance, which facilitates the implementation to conduct simulations. In this work, a HIF model based on the arc conductivity is used, which is developed by a first-order differential equation [4].

$$\frac{d\left(\ln g(t)\right)}{dt} = \frac{1}{\tau}\left(\frac{vi}{P} - 1\right) \quad (5)$$

where v and i represent the arc voltage and current, respectively; $g(t)$ is the arc conductance, $\tau(v, i)$ is the time constant, and $P(v, i)$ is the arc power in steady-state. Then, by taking τ as a constant and the steady-state power as $P = P_0 + v_0 i$, the solution to (5) can be obtained.

According to [4], the general equation to represent the arc conductance in the time domain is expressed by:

$$g(t) = G_0(1 - e^{-t/\tau}) \quad (6)$$

where $g(t)$ is the time-varying conductance and G_0 is the steady-state conductance. Due to the need to interface the non-linear conductance-resistance model with the standard models, in this work, the model is implemented with a non-linear resistance by using a block of a controlled current source through Matlab-Simulink software.
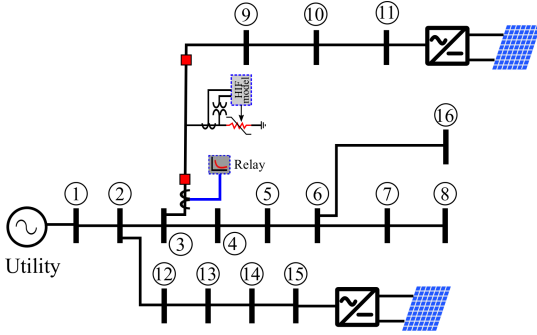
FIGURE 1. HIF model implemented in Matlab-Simulink.

C. HIFS ANALYSIS BASED ON THE HERMITE TRANSFORM

Figure 1 shows a test system to cope with the signal processing of HIFs in active distribution networks. The sampling frequency used is 6.4 kHz for a fundamental frequency of 50 Hz. A HIF was simulated between buses 3 and 9 of the test systems. In this case, Fig. 2a) depicts the HIF current at the fault point along the fault period. In addition, the corresponding voltage-current (V-I) characteristics are shown in Fig. 2b). Finally, the line currents seen by the protection devices are represented in Fig. 2c). In this case, a current transformer (CT) with a ratio of 100:5 was employed. Due to the current magnitudes of HIFs, the CT will not experience the saturation phenomenon.

Figure 3 depicts the HT coefficient for a typical HIF fault. Each resolution level corresponds to the HT coefficients according to the filter function defined by the Hermite polynomials. The HT coefficients at each resolution are normalized magnitudes where it can notice that the HT is suitable to reveal the underlying high frequency components when a HIF occurs. It is important to highlight that the calculation of the HT coefficients will permit the detection and classify HIFs in distribution grids with higher efficiency.

III. CLASSIFICATION APPROACH FOR HIGH IMPEDANCE FAULTS

A. FEATURE EXTRACTION

The effectiveness of any classifier to discriminate typical faults from high impedance faults depends on the feature extraction that can be carried out in the time or frequency domains. The feature extraction of high impedance faults is not an easy task since the current magnitudes may present small changes that can be interpreted as load variations [20]. As a consequence, HIFs require robust algorithms able to distinguish them from other fault types. One effective way to extract the most relevant characteristics of HIFs is commonly based on multiresolution approaches [18], [26]. In general, multiresolution analysis facilitates feature extraction because it provides information in time and frequency at different resolution levels. As a consequence, a suitable selection may help to enhance the effectiveness of any classifier.
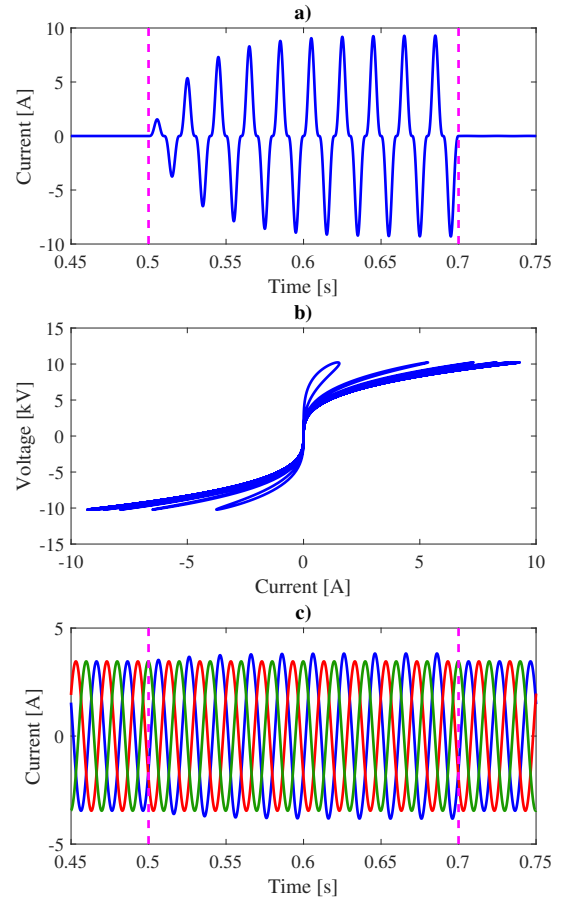
FIGURE 2. HIF in a distribution network: a) current, b) V-I characteristics, and c) line currents seen by the digital relay.

In this work, the feature extraction is performed through a Hermite transform-based multiresolution approach where it can obtain the high-frequency components of the analysed signals, HIFs and different types of faults in distribution networks. The analysis employs different resolution levels that allows identifying the most relevant transient characteristics, which are used to establish the feature extraction defined by statistical indexes as follows:

$$F_1 = \sqrt{\frac{1}{N-1} \sum_{k=1}^{N} (y_k - \mu)} \tag{7}$$

$$F_2 = \frac{1}{N} \sum_{k=1}^{N} |y_k| \tag{8}$$

$$F_3 = \frac{1}{N} \sum_{k=1}^{N} y_k^2 \tag{9}$$

$$F_4 = \frac{(1/N) \sum_{k=1}^{N} (y_k - \mu)}{(1/N) \left(\sum_{k=1}^{N} (y_k - \mu)^2 \right)^2} \tag{10}$$
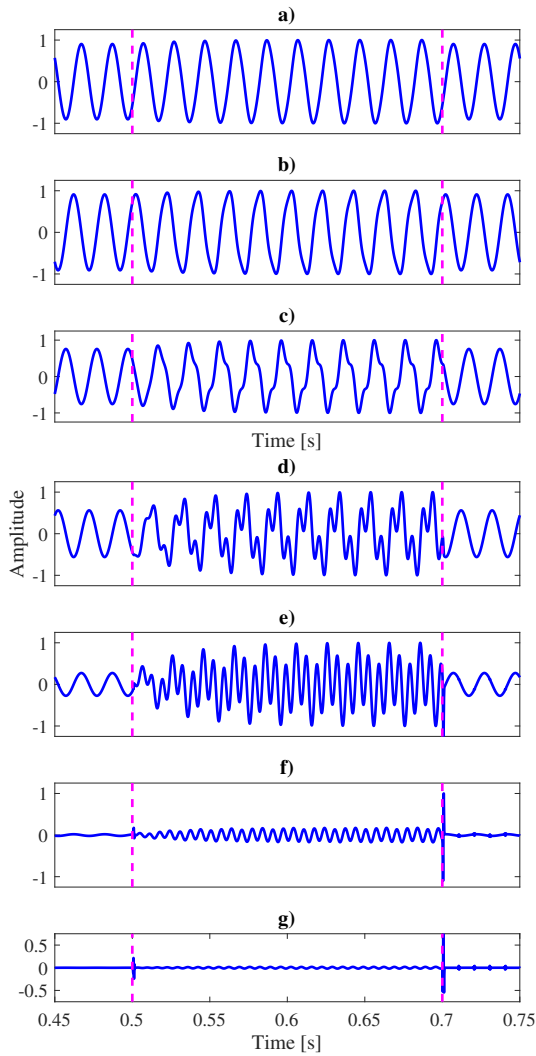
FIGURE 3. HIF signal processed by the HT: a) coefficients of order 0, b) coefficients of order 1, c) coefficients of order 2, d) coefficients of order 3, e) coefficients of order 4, f) coefficients of order 5, and g) coefficients of order 6.

where N is the number of samples, μ represents the average value, F_1 corresponds to the standard deviation, F_2 is the average absolute magnitude, F_3 stands for the average energy, F_4 represents the Kurtosis index.

B. PROPOSED APPROACH

This proposal introduces a new method to detect and classify HIFs as well as typical faults in distribution systems. The proposed approach is summarized in Fig. 4, which consists of six stages. First, the electrical signals are measured on the protected line by employing current transformers (CTs). Next, all measured signals I_{line} (I_a, I_b, and I_c) are processed by the HT to extract the high-frequency components. To this aim, the process consists in representing all transient frequency components in different resolution levels computing the convolution between any measured signal and the Hermite polynomials. Therefore, each current signal I_{line} will be represented by a matrix of N samples and L resolu-

tion levels $I_{HTC-line}$. In this work, the Gaussian derivatives from 1-st to 6-th are used according to the HT. Then, to distinguish HIFs from typical faults, a max-pooling process is carried out to reduce the transient information; for this purpose, it is suggested using a resolution level (or level of decomposition) multiple of three, this means that the max-pooling will generate a new matrix with N samples and $L/3$ resolution levels, and it is also computed the determinant for the resulting matrix so that the new signal $I_{HT-line}$ is represented by one dimension, that is, N samples. This signal $I_{HT-line}$ will store all transient components used to the feature extraction. Lastly, the feature extraction process is carried out that will define the inputs of the classifier. Finally, the complete data set is divided to conduct the training and validation stages of classification to distinguish HIFs from typical faults.

For better understanding, Fig. 5 shows the stages of the proposed approach. The line currents are processed using the HT, where the HT coefficients are employed to extract the most essential high-frequency components. Notice that this proposal faithfully captures the transient information produced by HIFs in distribution systems. For example, Fig. 5a) depicts the line currents (I_a, I_b, and I_c) where small changes in the current magnitudes occur at $t = 0.5$ s. Based on the proposed method, the processing of the HT coefficients permits to identify of the most relevant transient components, which is confirmed in Fig. 5b), both for the non-faulted phases (I_{HTa} and I_{HTb}) and the faulted phase I_{HTc}. Finally, the defined features are shown in Fig. 5c) which correspond to the faulted phase I_a just after processing the HT coefficients stored in I_{HTa}.

C. CLASSIFIERS

To deal with the classification of high impedance and typical faults, three different classifiers are used in this work such as: k-nearest neighbour (KNN), support vector machine (SVM) and artificial neural networks (ANNs).

1) K-nearest neighbour (KNN)

KNN is a supervised classifier based on a distance metric and K number of neighbours defined by the user [27]. For example, many training samples of any particular fault type, also known as a class, a new sample can be assigned to the class according to the most frequent K-nearest neighbours (KNNs). That is, the algorithm assigns the sample to the class among its KNNs, where K is an integer. In addition, to overcome bias in the class prediction due to unbalanced data, weight proportional to the inverse of the distance from the K neighbours is assigned to each class. In the process of creating a KNN classifier, K is an important parameter and different values will cause different performances, they impose a significant influence on the time and accuracy performance of the classification. For this work, K is 5 and the used metric was the Euclidean distance.
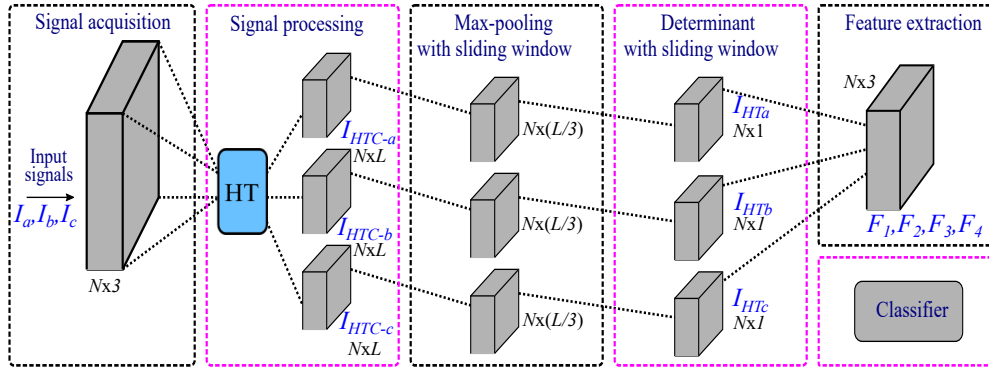
FIGURE 4. Schematic diagram of the proposed approach.
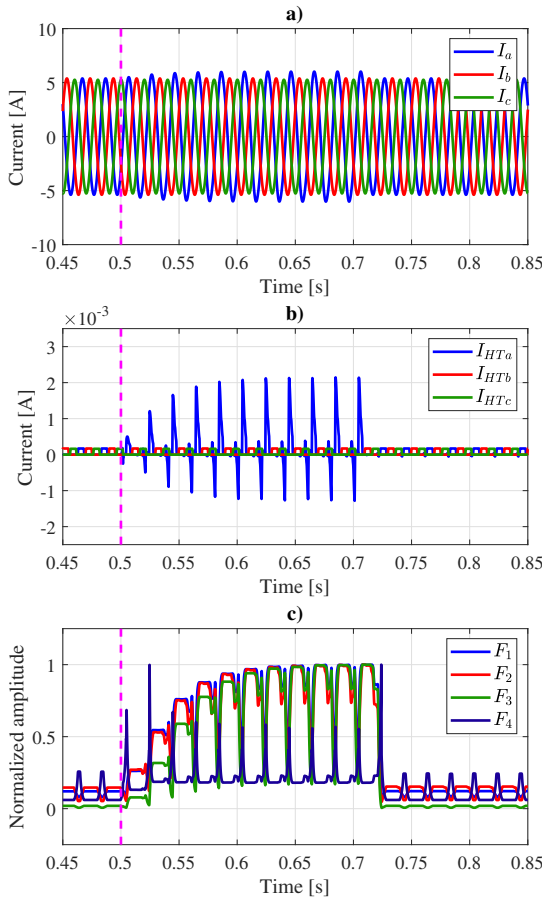
FIGURE 5. HIF simulated : a) line currents seen by the digital relay, b) transient components-based algorithm using HT, and c) features.

2) Support vector machine (SVM)

Support vector machine is a widely known algorithm for supervised learning. This classifier uses an objective function aiming at minimizing misclassification errors by maximizing the separation margin. It also separates classes by constructing a hyperplane in the high dimensional features as shown in Fig. 6.

For instance, in a two-class problem, the mapping consists
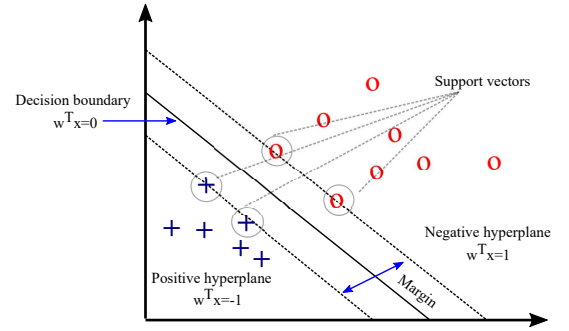
FIGURE 6. Support vector machine diagram.

of a two-stage dataset $(x_i y_i)_{i=0}^{N}$ with N data points where x_i is the training data, and y_i is the corresponding class, which takes values of +1 and -1. In this sense, the margin is the distance between the separating hyperplane and the training samples that are closest to the hyperplane, these are also called support vectors. The hyperplane separates both categories, and its equation is:

$$w^T x_i + b = 0 \qquad (11)$$

where ω represents the weight vector, and b is the bias parameter; both parameters determine the position of the hyperplane. In the training stage, the best values of these parameters are obtained such that they maximize the separation between both categories, obtaining the separation margin as $m = 2/\|m\|$. Therefore, the objective function will maximize the margin defined by the relation between m (margin value) and ω (weight values), that is, the solution allows obtaining these values, and the samples are classified correctly as [28]:

$$y^{(i)}(w_0 + w^T x^{(i)}) \geq 1, \forall_i \qquad (12)$$

Finally, the classification is carried out by separating all negative samples on one side of the hyperplane (first class), and the positive samples on the other side of the hyperplane (second class). Additionally, SVMs can be converted into a multivalued classifier using one to one method. In this work,

a Gaussian radial basis function (RBF) kernel is employed and a cross-validation procedure is carried out during the training of the data set used.

3) Artificial Neural Networks (ANNs)

An ANN classifier is widely used in machine learning, which has proven to be a powerful supervised learning algorithm because of its parallel processing, nonlinear mapping, and associative memory. Multilayer neural networks are able to produce robust diagnostics for different areas of electric power systems [29]. The method consists of a training stage, where the network weight parameters are tuned by means of back-propagation so that a cost function must be minimized. The equation shows an iterative process to update the weights through the back-propagation process.

$$w := w + \Delta w,$$
$$\Delta w = -\eta \bigtriangledown J(\omega) \quad (13)$$

where, w represents the weights, which are updated by taking a step in the opposite direction of the gradient $\bigtriangledown I(\omega)$. Besides, the gradient is multiplied by a factor known as the learning rate η .

In general, the learning rate balances the speed of the learning with the overshoot of the global minimum of the cost function, which is usually defined by the sum of square errors. Therefore, if the error is low, then the weights offer a better behavior. A graphical basic architecture of a single-layer neural network is shown in Fig. 7. For a multilayer scheme, the output is connected to the next layer and so on. In this application, 10 layers are used and the activation function corresponds to the cross-entropy.
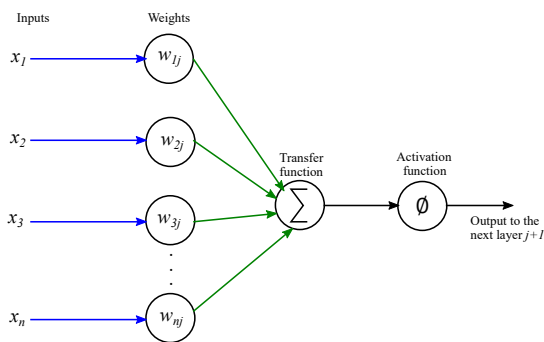
FIGURE 7. Single-layer neural network.

IV. RESULTS AND DISCUSSIONS

A. DISTRIBUTION GRID UNDER TEST

The detection and classification analyses are carried out by using the IEEE 33-bus test feeder, which is shown in Fig. The The detection and classification analysis are carried out by using the IEEE 33-bus test feeder, which is shown in Fig. 8. All simulations are carried out in Matlab/Simulink software by employing a sampling frequency of 6.4 kHz. All fault

scenarios are performed between buses 3 and 23, corresponding to the distribution line identified as L3-23. The data set includes non-fault scenarios, HIFs, and typical faults such as single-phase-to-ground, double-phase-to-ground, and three-phase-to-ground faults. The typical faults take into account different fault locations along the distribution line, several fault resistance, and different fault inception angles; different contact surfaces for HIFs are analysed considering variations in the electric arc's conductance. Besides, capacitor bank switching is simulated at bus 24, load changes of linear load are assessed at bus 25, and finally, a non-linear load is modelled at bus 29.

B. DETECTION BASED ON THE HT COEFFICIENTS

The proposed approach can be employed to cope with the HIF detection based on a sliding window analysis. In this case, the detection index is defined by the extracted features as follow:

$$\lambda(k) = N \times \left(\frac{F_1(k) + F_2(k) + F_3(k)}{3} \right) \times F_4(k) \quad (14)$$

To analyse the performance of the transient components-based algorithm, an analysis of several fault scenarios is carried out using the test system shown in Fig. 8. For example, a HIF is simulated taking into account a power electronic converter-based distributed generator (250 kW Photovoltaic system) at bus 25. In this case, a HIF was simulated at $t = 0.5$ s and its results are depicted in Fig. . From Fig. a), it can be noticed that the line currents in the abc reference frame show small changes in magnitude during the fault which was simulated at $t = 0.5$s. On the other hand, Fig. b) shows the most relevant transient information during the pre-fault, fault and post-fault periods. Notice that the proposed approach can disclose the underlying high-frequency components of the analysed signal which can be verified in Fig. b). After processing the HIF signal information, Fig. c) displays the results of the HIF detection according to the transient components-based algorithm.

To highlight the advantages of the proposed approach, a single-phase fault is simulated and its results are shown in Fig. 10. In this case, the fault is simulated at $t = 0.5$ s and the line currents observed by the protection devices are depicted in Fig. 10a). After processing the line currents, the most essential transient components are captured that will be used to extract the signal features in order to identify HIFs; these components for each line current are displayed in Fig. 10b) and the HIF detection corresponds to Fig. 10c). Therefore, a transient event is detected so to confirm that a HIF occurred, it is required at least one cycle of the fundamental frequency to avoid false classification results.

Capacitor switching may be one cause of false detection as well as load changes. Therefore, the proposed approach is examined considering the transient behaviour under non-fault conditions. For instance, Fig. 11 the response when a capacitor bank is energized at bus 24 (1.5 MVar). These
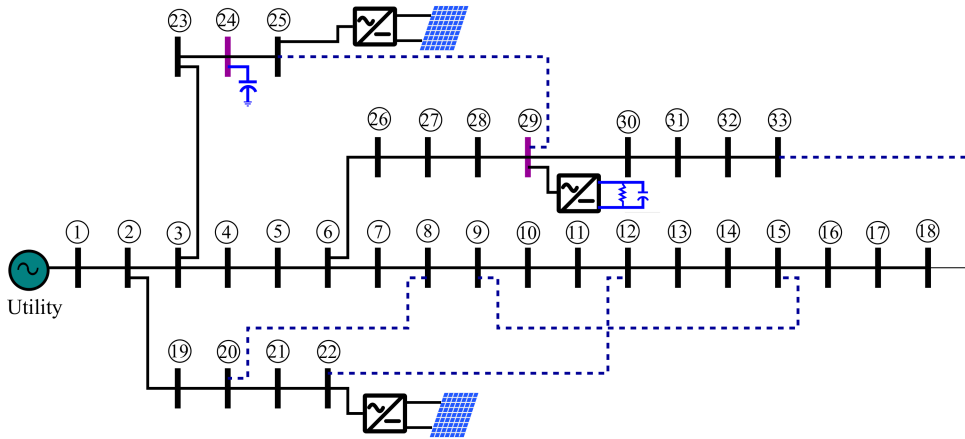
FIGURE 8. IEEE 33-bus test feeder.
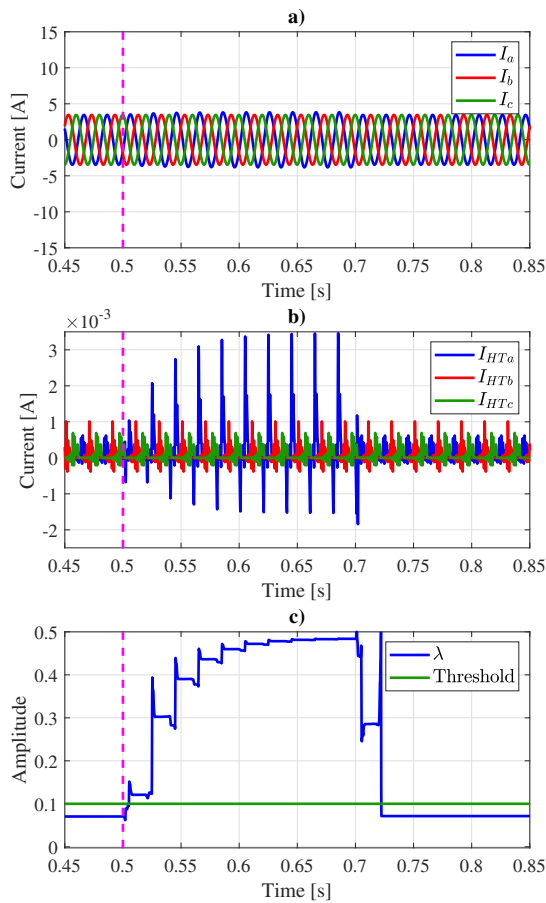
FIGURE 9. HIF with distributed generation: a) line currents and b) HT coefficients, and c) HIF detection using transient components-based algorithm.
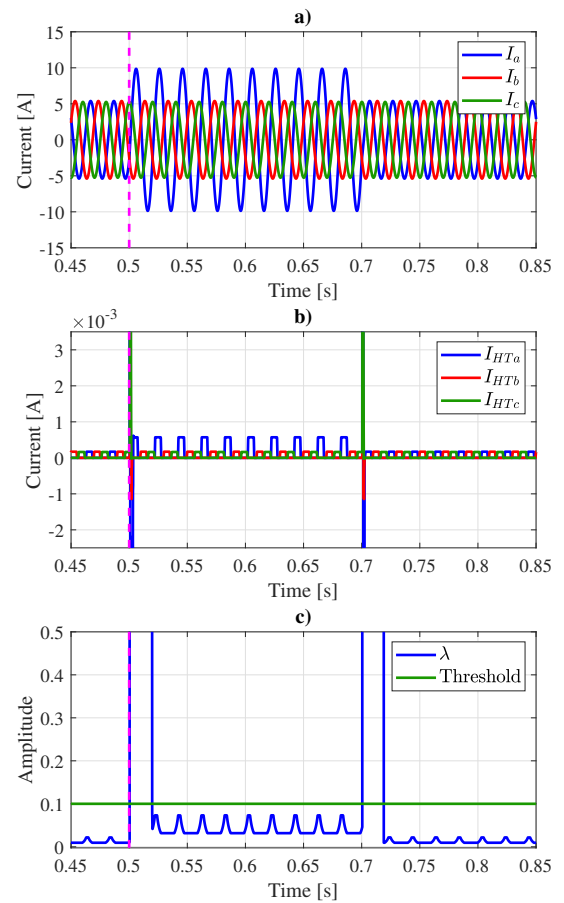
FIGURE 10. Single-phase fault with fault resistance of 100 Ω: a) line currents and b) HT coefficients, and c) HIF detection using transient components-based algorithm.

results correspond to an energization when the voltage (Phase A as a reference) is crossing by its maximum value, $t = 5.05$ s. The line currents in the abc reference frame are shown in Fig. 11a) and Fig. 11b) presents the results of the detection index computed by employing the HT coefficients. Notice that the transient response disappears during the first two cycles.

Therefore, this phenomenon may generate false classification results during the transient period, this means that after two cycles the transient components-based algorithm will offer good performance during the detection and classification of HIFs.
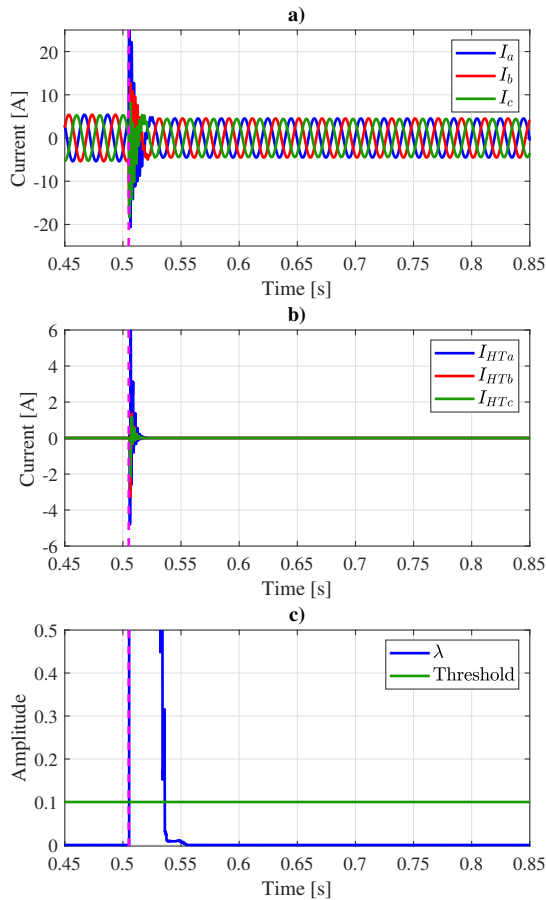
FIGURE 11. Capacitor switching: a) line currents and b) HT coefficients, and c) HIF detection using transient components-based algorithm.

FIGURE 12. Load change at bus 29: a) line currents and b) HT coefficients, and c) HIF detection using transient components-based algorithm.

Figure 12 shows the results during load changes. The change is simulated at bus 29 caused by a non-linear load. The non-linear load is energized at $t = 0.5$ s and its results are displayed in Fig. 12. In this case, a small change is taken into account, and the line currents seen by the digital protection device are shown in Fig. 12a), while the corresponding transient information is captured by processing the line currents using the HT which coefficients are represented in Fig. 12b). Notice that the load change presents significant differences along the time as shown in Fig. 12c), however, this event is correctly identified as a non-faulted condition.

Based on the results, the proposed method exhibits good performance during the fault detection and the detection time will depend on the sampling frequency used. In this case, the average time is 20.2 ms considering the system's frequency, 50 Hz. Before the average time, a HIF may not be correctly detected and can be classified as a non-fault condition. In consequence, the performance of the classifiers may also be affected. Therefore, to improve the detection and classification of HIFs, this work needs at least two cycles regarding the fundamental frequency, that is, higher accuracy and reliability entail a longer detection time so that for HIFs the accuracy will be important to avoid additional problems

based on the complex nature of the electric arc phenomenon.

C. CLASSIFICATION RESULTS

Table 1 depicts the results reached by the classification process. Based on the results, notice that the most promising classifier is KNN because this presents better performance than SVM and ANN. In general, the effectiveness of classifiers will especially depend on the data set used for training, and the feature extraction process. As a consequence, if there is a data set substantially full of significant information, the classification results will be more accurate. Table 1 presents the obtained results applying the proposed method. In addition, for comparison purposes the studied faults were also processed by the DWT using 6 decomposition levels using the mother wavelet Daubechies 4 (Db4). Results show that both signal processing techniques present small differences when the KNN classifier is applied where the most significant discrepancy appears with the other two classifiers. On the other hand, Fig. 13 presents the confusion matrix following the proposed approach by using the KNN classifier. From Fig. 13, notice that the false-positives of the HIFs are identified as non-fault conditions.

Another subject to analyse the metrics of any classifier

TABLE 1. Proposed approach using HT and DWT

Classifier	Accuracy (%)	
	DWT	HT
SVM	94.7122	98.1538
KNN	98.8191	99.2722
ANN	84.7286	92.0189

Target class

	C1	C2	C3	C4	C5	Condition
C1	4864	0	0	0	0	Non-fault
C2	0	4863	1	0	0	1Fg
C3	0	77	4787	0	0	2Fg
C4	0	76	0	4788	0	3Fg
C5	23	0	0	0	4841	HIF

FIGURE 13. Confusion matrix using HT and KNN with a balanced data set.

Target class

	C1	C2	C3	C4	C5	Condition
C1	100	0	0	0	0	Non-fault
C2	0	496	4	0	0	1Fg
C3	0	6	794	0	0	2Fg
C4	0	6	0	194	0	3Fg
C5	3	0	2	0	45	HIF

FIGURE 14. Confusion matrix using HT and KNN with an unbalanced data set.

scales. In conclusion, the proposed method presents better performance for the discussed scenarios.

TABLE 2. Proposed approach using an unbalanced data set.

Classifier	Accuracy (%)	
	DWT	HT
SVM	96.3636	97.5152
KNN	98.8182	98.7273
ANN	96.9697	96.9697

is its behaviour when an unbalanced data set is employed. For example, in this application, a critical condition will be when the protection systems are not capable of detecting any condition of HIFs, that is, the fault could be classified as a non-fault scenario. This represents a critical scenario compared to misclassification resulting in other fault types, for example, a double-phase fault which is identified as a three-phase fault. In this sense, an unbalanced data set is employed to assess the proposed method whose results are shown in Table 2 and Fig. 14. It can be noticed that the results present significant changes in the classifiers used as is shown in Table 2. However, the best results correspond to the KNN classifier while the ANN improves in comparison with the results shown in Table 1. Besides, the SVM offers small changes in both scenarios when a balanced and an unbalanced data set is employed.

Finally, the confusion matrix obtained by the developed method is depicted in Fig. 14. Notice that HIFs produce false positives identified as non-fault events and double-phase faults. This means that if a HIF is classified as a fault (no matter which fault type), this will be better for the system than a HIF will be identified as a non-fault event. Finally, the comparison results after applying the DWT show that both techniques generate similar results, where the better results are achieved by the KNN classifier since all results are very close to those produced by the proposed approach. In terms of complexity both DWT and HT demand a similar computational burden. The advantage of the HT relies on the basis functions that are better suited to detect signal changes at multiple resolutions since they consist of Gaussian derivatives of different orders at different scales, whereas the DWT has a single basis function (mother wavelet) at different

V. CONCLUSION

A new method for fault detection and classification of HIFs in distribution systems was proposed. This proposal included a methodology based on the high-frequency components, which are obtained by using a multiresolution approach according to the HT. All mathematical fundamentals were addressed and the method was proved under different transient scenarios to demonstrate its performance during the discrimination of HIFs from other types of faults. In addition, the non-fault transient events were discussed to show that high-frequency components produced by the non-linear load changes will depend on the load capacity. This means that larger load changes (non-linear load) may produce misclassification depending on the harmonic content. Based on the results, the transient components-based method exhibited good performance and effectiveness for different analysed scenarios by exploiting the advantages of the HT, where the HT coefficients played a key role to extract the most essential information during the transient period of the electrical signals. It was noticed that the Hermite transform presents several advantages with respect the DWT due to the localization properties of the Gaussian function and its derivatives of the HT, which retain the most relevant transient information according to the statistical indexes used. Finally, different classifiers such as SVM, KNN, and ANN showed good accuracy taking as inputs the statistical indexes defined by the HT coefficients. The obtained results were also compared with the DWT where it was found that KNN offered better performance than the other tested classifiers.

REFERENCES

[1] O. Gashteroodkhani, M. Majidi, and M. Etezadi-Amoli, "Fire hazard mitigation in distribution systems through high impedance fault detection," *Electric Power Systems Research*, vol. 192, p. 106928, 2021.

[2] R. B. Grimaldi, T. S. Chagas, J. Montalvão, N. S. Brito, W. C. dos Santos, and T. V. Ferreira, "High impedance fault detection based on linear prediction," *Electric Power Systems Research*, vol. 190, p. 106846, 2021.

[3] M. Biswal, S. Ghore, O. P. Malik, and R. C. Bansal, "Development of time-frequency based approach to detect high impedance fault in an inverter interfaced distribution system," *IEEE Transactions on Power Delivery*, pp. 1–1, 2021.

[4] V. Torres, J. Guardado, H. Ruiz, and S. Maximov, "Modeling and detection of high impedance faults," *International Journal of Electrical Power & Energy Systems*, vol. 61, pp. 163–172, 2014.

[5] S. Chakraborty and S. Das, "Application of smart meters in high impedance fault detection on distribution systems," *IEEE Transactions on Smart Grid*, vol. 10, no. 3, pp. 3465–3473, 2019.

[6] J. R. Macedo, J. W. Resende, C. A. Bissochi Jr, D. Carvalho, and F. C. Castro, "Proposition of an interharmonic-based methodology for high-impedance fault detection in distribution systems," *IET Generation, Transmission & Distribution*, vol. 9, no. 16, pp. 2593–2601, 2015.

[7] D. A. Gadanayak and R. K. Mallick, "Interharmonics based high impedance fault detection in distribution systems using maximum overlap wavelet packet transform and a modified empirical mode decomposition," *International Journal of Electrical Power & Energy Systems*, vol. 112, pp. 282–293, 2019.

[8] F. B. Costa, B. A. Souza, N. S. D. Brito, J. A. C. B. Silva, and W. C. Santos, "Real-time detection of transients induced by high-impedance faults based on the boundary wavelet transform," *IEEE Transactions on Industry Applications*, vol. 51, no. 6, pp. 5312–5323, 2015.

[9] F. B. Costa, "Boundary wavelet coefficients for real-time detection of transients induced by faults and power-quality disturbances," *IEEE Transactions on Power Delivery*, vol. 29, no. 6, pp. 2674–2687, 2014.

[10] W. C. Santos, F. V. Lopes, N. S. D. Brito, and B. A. Souza, "High-impedance fault identification on distribution networks," *IEEE Transactions on Power Delivery*, vol. 32, no. 1, pp. 23–32, 2017.

[11] S. Roy and S. Debnath, "Psd based high impedance fault detection and classification in distribution system," *Measurement*, vol. 169, p. 108366, 2021.

[12] K. Swarna, A. Vinayagam, M. Belsam Jeba Ananth, P. Venkatesh Kumar, V. Veerasamy, and P. Radhakrishnan, "A knn based random subspace ensemble classifier for detection and discrimination of high impedance fault in pv integrated power network," *Measurement*, vol. 187, p. 110333, 2022.

[13] K. Sekar and N. K. Mohanty, "Data mining-based high impedance fault detection using mathematical morphology," *Computers & Electrical Engineering*, vol. 69, pp. 129–141, 2018.

[14] M. Kavi, Y. Mishra, and M. D. Vilathgamuwa, "High-impedance fault detection and classification in power system distribution networks using morphological fault detector algorithm," *IET Generation, Transmission & Distribution*, vol. 12, pp. 3699–3710(11), August 2018.

[15] H. Lala and S. Karmakar, "Detection and experimental validation of high impedance arc fault in distribution system using empirical mode decomposition," *IEEE Systems Journal*, vol. 14, no. 3, pp. 3494–3505, 2020.

[16] M. Sarlak and S. Shahrtash, "High impedance fault detection using combination of multi-layer perceptron neural networks based on multi-resolution morphological gradient features of current waveform," *IET Generation, Transmission & Distribution*, vol. 5, pp. 588–595(7), 2011.

[17] J. G. Sousa Carvalho, A. Rocha Almeida, D. D. Ferreira, B. F. dos Santos, L. H. Pereira Vasconcelos, and D. de Oliveira Sobreira, "High-impedance fault modeling and classification in power distribution networks," *Electric Power Systems Research*, p. 107676, 2021.

[18] D. P. S. Gomes, C. Ozansoy, and A. Ulhaq, "High-sensitivity vegetation high-impedance fault detection based on signal's high-frequency contents," *IEEE Transactions on Power Delivery*, vol. 33, no. 3, pp. 1398–1407, 2018.

[19] A. Ghaderi, H. A. Mohammadpour, H. L. Ginn, and Y. Shin, "High-impedance fault detection in the distribution network using the time-frequency-based algorithm," *IEEE Transactions on Power Delivery*, vol. 30, no. 3, pp. 1260–1268, 2015.

[20] M. Eslami, M. Jannati, and S. S. Tabatabaei, "An improved protection strategy based on pcc-svm algorithm for identification of high impedance arcing fault in smart microgrids in the presence of distributed generation," *Measurement*, vol. 175, p. 109149, 2021.

[21] K. Sarwagya, "High-impedance fault detection in electrical power distribution systems using moving sum approach," *IET Science, Measurement & Technology*, vol. 12, pp. 1–8(7), January 2018.

[22] L. U. Iurinic, A. R. Herrera-Orozco, R. G. Ferraz, and A. S. Bretas, "Distribution systems high-impedance fault location: A parameter estimation approach," *IEEE Transactions on Power Delivery*, vol. 31, no. 4, pp. 1806–1814, 2016.

[23] J. Martens, "The hermite transform-theory," *IEEE Transactions on Acoustics, Speech, and Signal Processing*, vol. 38, no. 9, pp. 1595–1606, 1990.

[24] A. P. Witkin, "Scale-space filtering," in *Proceedings of the Eighth International Joint Conference on Artificial Intelligence-Volume 2*, ser. IJCAI'83. San Francisco, CA, USA: Morgan Kaufmann Publishers Inc., 1983, p. 1019–1022.

[25] J. L. Silvan-Cardenas and B. Escalante-Ramirez, "The multiscale hermite transform for local orientation analysis," *IEEE Transactions on Image Processing*, vol. 15, no. 5, pp. 1236–1253, 2006.

[26] M. Mishra and R. R. Panigrahi, "Taxonomy of high impedance fault detection algorithm," *Measurement*, vol. 148, p. 106955, 2019.

[27] O. Yaman, "An automated faults classification method based on binary pattern and neighborhood component analysis using induction motor," *Measurement*, vol. 168, p. 108323, 2021.

[28] P. Ghalyani and A. Mazinan, "Performance-based fault detection approach for the dew point process through a fuzzy multi-label support vector machine," *Measurement*, vol. 144, pp. 214–224, 2019.

[29] H. A. Illias, X. R. Chai, and A. H. Abu Bakar, "Hybrid modified evolutionary particle swarm optimisation-time varying acceleration coefficient-artificial neural network for power transformer fault diagnosis," *Measurement*, vol. 90, pp. 94–102, 2016.

DANIEL GUILLEN (Member, IEEE) received the B.Eng. degree in electrical engineering from the Instituto Tecnologico de Morelia, Mexico, in 2007, and the M.Sc. and Ph.D. degrees in electrical engineering from the Universidad Autonoma de Nuevo Leon, Mexico, in 2010 and 2015, respectively. He was with the National Center of Energy Control (CENACE-Mexico) conducting interconnection studies of renewable energy, such as solar and wind power plants, from 2015 to 2016. He was an Associate Professor with the Universidad Nacional Autonoma de Mexico, from 2016 to June 2018. His research interests include power system modeling, power system protection, wide-area monitoring, signal processing, and transient analysis. He is currently with the Tecnológico de Monterrey and is member of the National Research System, National Council of Science and Technology (CONACyT-Mexico), level 1 (SNI-1).

JIMENA OLVERES received her B.S. degree in Biomedical Engineering from Universidad Iberoamericana in México city, a Master in Engineering and a Ph.D. in Computer Science from UNAM. Her research areas include computational models for image processing, machine learning for computer vision, specializing in medical image analysis.

VICENTE TORRES-GARCIA (Senior Member, IEEE)

BORIS ESCALANTE-RAMIREZ received a Ph.D. from the Technical University of Eindhoven (1992). His research areas include computational models for image processing and computer vision.

• • •